



Synthesis and Characterizations of $Ce_{0.5}Sr_{0.5}Co_{0.8}Fe_{0.2}O_{3-\delta}$ (CSCF) Solid Oxide Fuel Cell Cathode Material by Sol-Gel method

Beyene Tesfaw Ayalew*¹, P.Vijay Bhaskar Rao¹

¹Department of Physics, Wollega University, Nekemte, Ethiopia

Abstract : $Ce_{0.5}Sr_{0.5}Co_{0.8}Fe_{0.2}O_{3-\delta}$ (CSCF) powders had been synthesized by Sol-Gel method. To get appropriate results, sintering temperature, heating and cooling rates and particle sizes were controlled. The prepared samples were calcined at 750°C for 3hrs and 900 °C for 5hrs. The sintered samples were characterized using XRD, SEM with EDS, Raman spectroscopy and TGA-DTA. XRD results showed the perovskite phase with average crystallite size of 26.57nm, density of 90.07%, lattice parameter 5.42293Å and cell volume of 159.47813Å³. Raman spectroscopy proved the existence of lattice vibrations with broader peaks at shoulders of 505.11cm⁻¹, 427.76cm⁻¹, 1455.30cm⁻¹, 434.04cm⁻¹ and 925.21cm⁻¹. TGA-DTA results gave information there were weight losses three times at 124.18°C, 330°C and 600°C.

Keywords : X-ray diffractometer, Density, Sol-Gel, $Ce_{0.5}Sr_{0.5}Co_{0.8}Fe_{0.2}O_{3-\delta}$.

1. Introduction

Using fuel cells as energy sources causes environmental issues by affecting the atmosphere. These environmental issues affect human life which leads to the innovation of alternative energy sources fuel cell. Fuel cells are electrochemical devices that convert the chemical energy of a reaction directly in to electrical energy. From different categories of fuel cells, the current attention is gone toward solid oxide fuel cells. ref----. Solid oxide fuel cell (SOFC) is an electrochemical device that changes chemical energy directly into electricity and heat by electrochemical reactions on the two electrodes separated by an oxide ion conducting electrolyte.

Even though SOFC is currently be a focus because of its high potential for power generation, there is an obstacle to commercializing SOFCs because of their cost which comes from high operating temperature. There is significant interest in lowering the operating temperature as well to exclude the potential problem coming from the sintering of electrode particles over time (Ormerod, 2003). Perovskite type cathode materials have been widely studied as cathode materials for SOFCs because of the possibility of both A-site and B-site doping. Their structure offers wide flexibility to improve the properties of materials, such as catalytic activity, chemical stability and thermal property (Yokokawa and Horita, 2003).

Widely used cathode material is strontium doped lanthanum manganite ($\text{La}_{1-x}\text{Sr}_x\text{MnO}_3$) (LSM) in high temperature SOFC (Muneeb, et al., 2009; Chunwen, Rob, & Justin, 2010). It is interconnected to manganite family of perovskites in which lanthanum is partially replaced with strontium. If there is excess lanthanum or strontium oxide, insulating phases like $\text{La}_2\text{Zr}_2\text{O}_7$ and SrZrO_3 is formed due to its interaction with yttria stabilized zirconia which leads towards poor performance. Nowadays, researchers are focused on SOFC devices capable of operating within an intermediate temperature (IT) range (500–700 °C). In this range, the main polarization losses occur on the cathode. $\text{La}_{0.8}\text{Sr}_{0.2}\text{MnO}_{3-\delta}$ (LSM), a commonly used cathode material within higher temperature ranges, exhibits high polarization resistance below 800 °C (Mosiałek, Dudek, Michna, Tatko, Kędra, & Zimowska, 2014).

The ferrite cathode material $\text{La}_{1-x}\text{Sr}_x\text{Co}_y\text{Fe}_{1-y}\text{O}_3$ (LSCF) is compatible with ceria based electrolyte and shows low resistance losses while being mixed ionic and electronic conductor (Wincewicz & Cooper, 2005). The electronic conductivity of LSCF decreases with increasing Fe Content (petric & Tietz, 2000). It has low power loss at lower temperature and less susceptibility to poisoning by chromium (Ullmann, 2000). The compound $\text{Ba}_{0.5}\text{Sr}_{0.5}\text{Co}_{0.8}\text{Fe}_{0.2}\text{O}_3$ has large thermal expansion coefficient (TEC) and has high oxygen ion mobility. Therefore, its use is minimal, and also shows high degradation for CO_2 containing atmospheres (Kuang & Easler, 2007). The compositions $\text{La}_{0.84}\text{Sr}_{0.16}\text{Co}_{0.3}\text{Fe}_{0.7}\text{O}_3$ (LSCFe7) and $\text{La}_{0.84}\text{Sr}_{0.16}\text{Co}_{0.7}\text{Fe}_{0.3}\text{O}_3$ (LSCFe3) prepared by solid state reaction and had densities of 91% and 93% respectively with a porosity of 7-9%; it has little effect on the electrical and electrochemical measurements. (Maguire, Gharbage, Marques, & Labrincha, 2000).

$\text{La}_{1-x}\text{Sr}_x\text{Fe}_{1-y}\text{Co}_y\text{O}_3$ (LSCF) shows good electrical conductivity, high oxygen surface exchange coefficient, and good oxygen self-diffusion coefficient between 600 and 800°C. The oxygen self-diffusion coefficient of LSCF is $2.6 \times 10^{-9} \text{cm}^2 \text{s}^{-1}$ at 500°C, which is better in performance to that of $\text{La}_{0.8}\text{Sr}_{0.2}\text{MnO}_3$ which has oxygen self-diffusion coefficient of $10^{-12} \text{cm}^2 \text{s}^{-1}$ at 1,000 °C (Dusastre & Kilner, 1999; Shao & Sossina, 2004). LSCF6428 was synthesized by microwave assisted sol-gel method and has a resistance of 0.17–0.2Ω in the range of temperature from 580–700°C (Mai, Ha, & Thang, 2016). Lanthanum strontium cobaltite (LSCO) for low and intermediate temperature SOFCs synthesized by sol-gel method gives lowest area specific resistance (ASR) of $3.52 \Omega \text{cm}^2$ at 800°C (Bajinath, Tiwari, & Basu, 2017).

For the last few years, $\text{Ba}_{1-y}\text{Sr}_y\text{Co}_{1-x}\text{Fe}_x\text{O}_3$ (BSCF) cathodes gained an increasing attention as a new cathode material for intermediate temperature SOFC applications (Holtappels, Vogt, & Graule, 2005). Due to the high activity for oxygen incorporation and moderate activity for hydrocarbon oxidation, BSCF is suitable for being applied as cathodes in single-chamber fuel cells operated with propane (Shao, Yang, Cong, Dong, Tong, & Xiong, 2001) or methane (Shao & Sossina, 2004). The electronic conductivity of LSCF is 215.58Scm^{-1} at 823K and it is higher than BSCF with a lower electronic conductivity 14.87Scm^{-1} at 773K (Jun, Yoo, Gwon, Shin, & Kim, 2013). The thermal expansion coefficient (TEC) of BSCF is much larger than the TEC of LSCF (Zhou, Ran, & Shao, 2009; Kuhn, Hashimoto, Sato, Yashiro, & Mizusaki, 2013). Although BSCF cathode material shows excellent electrochemical performance, the obvious disadvantage of BSCF is the high TEC, with a value of $20 \times 10^{-6} \text{K}^{-1}$ between 50°C and 1000°C (Wei, et al., 2006).

So the researcher is attempting to characterize the $\text{Ce}_{0.5}\text{Sr}_{0.5}\text{Co}_{0.8}\text{Fe}_{0.2}\text{O}_{3-\delta}$ (CSCF) cathode materials for Solid Oxide Fuel Cell by Sol-Gel method and study the structure, morphology, and TG-DTA results by analyzing the XRD, SEM, RAMAN and TG-DTA studies.

2. Experimental

2.1 Materials preparation method

Powders of Cerium nitrate hexahydrate ($\text{Ce}(\text{NO}_3)_2 \cdot 6\text{H}_2\text{O}$), Strontium nitrate ($\text{Sr}(\text{NO}_3)_2$), Cobalt nitrate hexahydrate ($\text{Co}(\text{NO}_3)_2 \cdot 6\text{H}_2\text{O}$) and hydrated Iron nitrate ($\text{Fe}(\text{NO}_3)_3 \cdot 9\text{H}_2\text{O}$) are grade sigma-Aldrich chemicals were used. The compound powders were synthesized by sol-gel method. The individual nitrates of precursor powders were mixed together by weighing stoichiometrically with a digital microbalance and dissolved in distilled water. Stoichiometric amount of citric acid was dissolved in the minimal amount of distilled water and mixed with the solution of metal nitrates by continuously stirring with a magnetic stirrer without heat. To avoid the appearance of hydroxides and base salts at higher pH values, the pH was adjusted to ~7. After the pH was adjusted the solution was slowly heated for 5hrs at 80°C over a temperature controlled magnetic stirrer with a

hot plate until the solution become a viscous like solid called gel. After the gel was formed stirring is stopped and continuing heating until it becomes a black ash.

The black ash was grinded with agate mortar for 1hr continually and small amount of powder was taken for TGA-DTA measurement to decide the sintering temperature of the sample and to study the thermal properties. Then the rest powder was putted in furnace for 3hrs at 750°C for pre-sintering. The pre-sintered powder again grinded for 1hr with agate mortar. The powder was made pellets by adding a polyvinyl alcohol gel for binding purpose. The pellets were made by using a hydraulic press with stainless steel die by applying a load of 12 ton for one minute for characterizations. At the end, the prepared pellets were sintered at 900°C for 5hrs to get the final composition and the desired pure phase perovskite before characterization and measurement.

During sintering, sintering temperature, atmosphere, heating and cooling rates, impurity concentrations and particle size must be controlled to obtain appropriate results. Since the sintering process has an influence on the microstructure of the resulting ceramic, the pressed pellets were sintered in a high temperature furnace in a closed alumina crucibles. The cooling rate also has a strong influence on the electrical property of the ceramics. The procedures had been repeated many times to get the highest purity crystalline phases of CSCF.

2.2 Method of Data Analysis

The analysis of the samples were carried out using X-ray diffractometer (XRD) for crystalline phase identification, Raman spectroscopy for vibrational, rotational, and other low-frequency mode studies of the material, Scanning electron microscopy (SEM) for surface morphology, Energy Dispersive Spectroscopy (EDS) for quantifying chemical composition at sub micron length scales and TGA-DTA for analyzing thermal properties.

3. Results and Discussions

3.1 X-ray Diffraction (XRD)

X-ray diffraction had been done to study the crystalline structure of the samples. X-ray diffraction data was taken by Xpert Philips XRD using Cu – K α radiation with a wave length of $\lambda=0.1542\text{nm}$ at a scanning rate of $2^\circ/\text{min}$ with a Cu anode of 40kv and 30mA. Scanning was taken for 2 θ values of ranging from 20° to 80° . From XRD patterns lattice parameters were calculated using UnitCellWin software. The average size of particles was calculated from the peak broadening using the Scherer formula using XRD data. The XRD pattern of sample $\text{Ce}_{0.5}\text{Sr}_{0.5}\text{Co}_{0.8}\text{Fe}_{0.2}\text{O}_{3-\delta}$ is given in figure 1 b

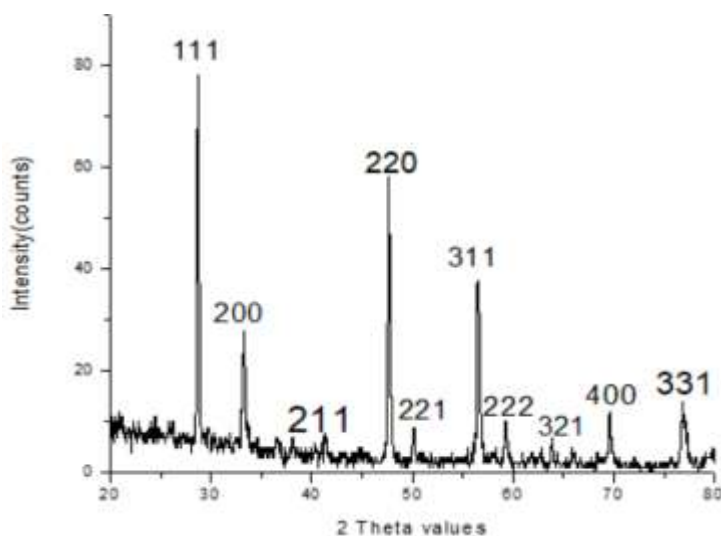


Figure 1: X-ray diffraction pattern for $\text{Ce}_{0.5}\text{Sr}_{0.5}\text{Co}_{0.8}\text{Fe}_{0.2}\text{O}_{3-\delta}$ sample

As it is observed from XRD pattern sintered at 900°C, Pure Perovskite phase was obtained. Even though the peak is obtained at this temperature, we get more pure peaks at temperatures between 1000°C and 1200°C; because at these temperatures almost all the impurities go out. The crystal structure is cubic and the average crystallite size of nano particles were calculated from XRD pattern peaks by using Scherer's formula and it is found to be was 26.57nm. Using the sharp peaks of XRD patterns, the crystalline nature of the sample was calculated and the value of lattice parameters to be $a = 5.42293\text{\AA}$ and cell volume of $V = 159.4781\text{\AA}^3$.

XRD patterns confirm the presence of a single-phase Perovskite structure containing cerium doping level up to 15% in A-site. As the concentration of cerium exceeds 15%, a small peak due to unreacted CeO_2 appears and its intensity increases with increment of cerium doping (Choi, Fuller, Davis, Wielgus, & Ozkan, 2012). From the X-ray density and experiment done for pellets in xylene, the value of experimental density was 5.40913gr/cm^3 and x-ray density was 6.00524gr/cm^3 respectively. The percentage density and porosity were 90.07% and 9.93% respectively. As observed from the result the material is porous and it is permeable for the flow of oxygen ions in to the triple phase boundary (TPB) and to the electrolyte.

3.2 Scanning Electron Microscopy (SEM)

Scanning electron microscopy is a technique used to investigate the microstructure of the samples prepared in this work. By using a high resolution SEM, the sample was analyzed to see the microstructure of the synthesized sample and to relate them with physical behaviors of the particles as a cathode material. As it is clearly seen from figure 2, the crystal consists of a periodic arrangement of the unit cell into a lattice. The unit cell can contain a single or more atoms in a fixed arrangement. It exhibited complete densification with a presence of pores on the surface. Grain boundaries are visible and the grain sizes are clearly increased. If the sintering temperature is increased, complete densification and posterior grain growth got and all metals are forced into the crystal network.

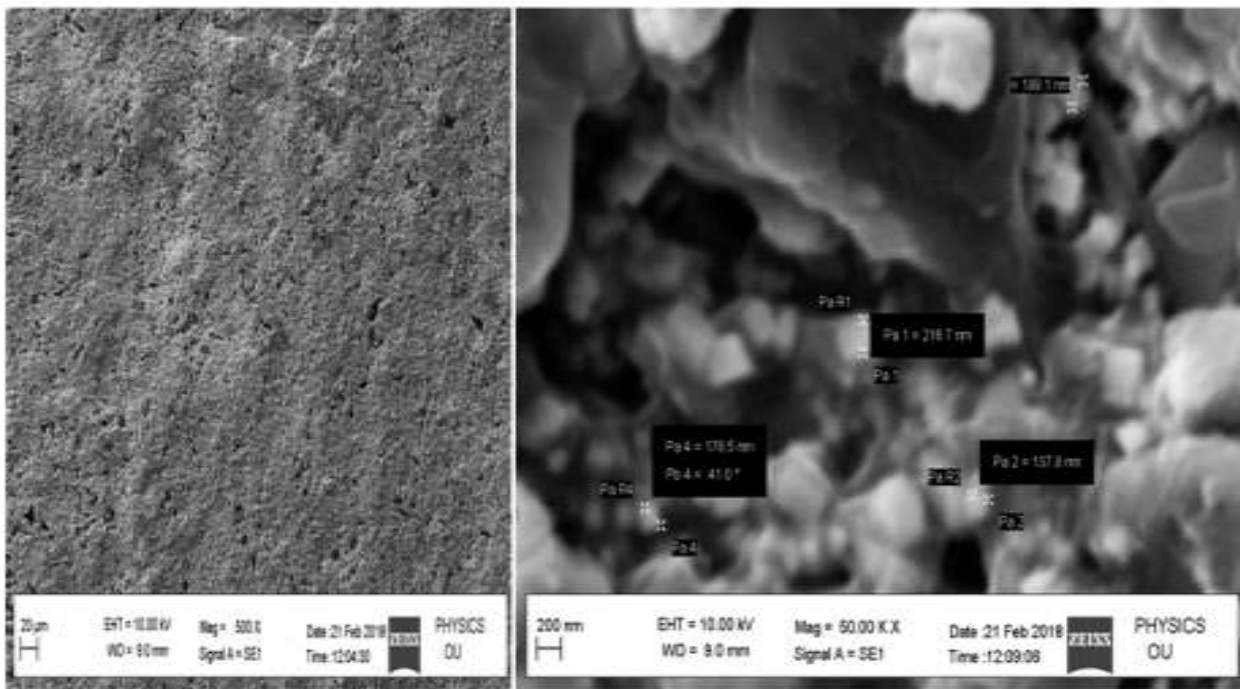


Figure 2: SEM pictures $\text{Ce}_{0.5}\text{Sr}_{0.5}\text{Co}_{0.8}\text{Fe}_{0.2}\text{O}_{3-\delta}$ sample at different magnifications

3.3 Energy Dispersive x-ray Spectroscopy (EDS) Analysis

EDS has been performed to ensure about the uniform distribution through the sample. Elemental maps of elements provide a visual illustration of their relative spatial distribution in the region corresponding to the micrograph. From the results of EDS showed in figure 3, the sample had the required elemental composition with their proportional weight percentage.

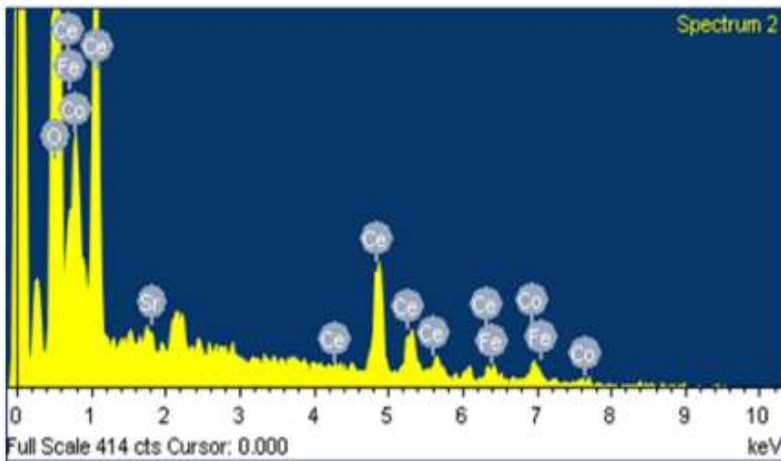


Figure 3: Energy Dispersive x-ray Spectroscopy spectrum for $\text{Ce}_{0.5}\text{Sr}_{0.5}\text{Co}_{0.8}\text{Fe}_{0.2}\text{O}_{3-\delta}$

3.4 Raman Spectroscopy Analysis

Raman spectroscopy is a form of vibrational spectroscopy in which the information obtained from Raman spectrum is related to vibrational modes of a molecule or the lattice phonon modes of a crystal. Raman spectroscopy is capable to distinguish the amorphous and crystalline state of materials much more precisely than the x-ray diffraction (Cavallaro, et al., 2018). As it was seen from figure 4, the sample was Raman-active and exhibits five peaks. The peaks are broader and contain a shoulder at 505.11cm^{-1} , 427.76cm^{-1} , 1455.30cm^{-1} , 434.04cm^{-1} and 925.21cm^{-1} respectively due to the presence of oxygen vacancies. A perfect cubic Perovskite has no Raman active phases. Since the sample was Raman active as seen from the figure it explains the tendency for these composition there is a distortion in a crystal structure and oxygen vacancies were formed due to doping.

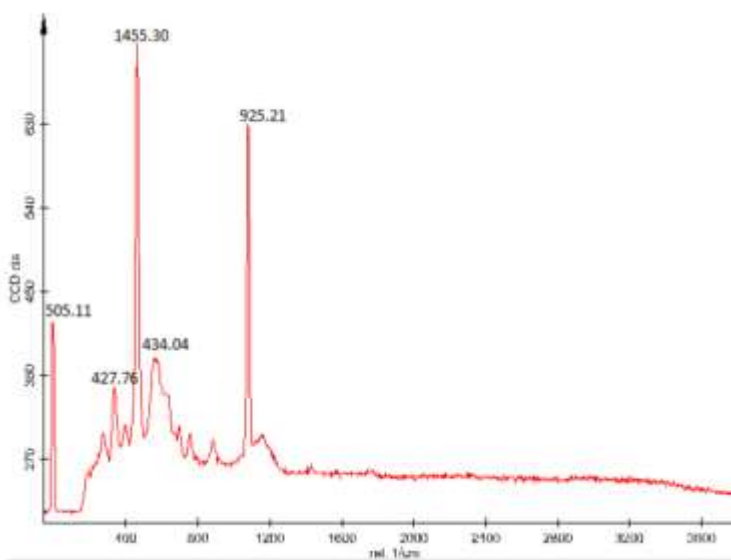


Figure 4: Raman spectra of $\text{Ce}_{0.5}\text{Sr}_{0.5}\text{Co}_{0.8}\text{Fe}_{0.2}\text{O}_{3-\delta}$ sample for SOFC cathode materials

3.5 Results of Thermal Analysis (TGA-DTA)

TGA-DTA is performed to determine changes in weight in relation to change in temperature. Such analysis relies on a high degree of precision weight, temperature and temperature change. The synthesized samples are placed on the platinum pan that is suspended from the analytical balance located outside the furnace chamber of the instrument TGA Q500 V20.13Build 39. The balance is zeroed and the sample cup is heated up from room temperature to 800°C .

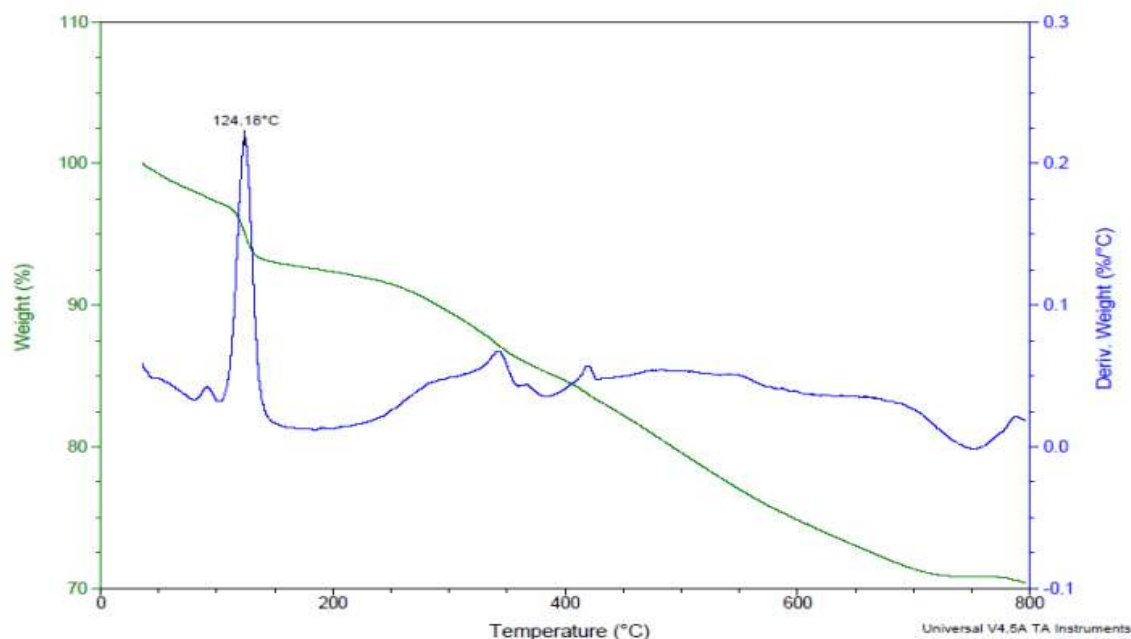


Figure 5: Thermo gravimetric (TGA-DTA) analysis for CSCF sample

Powders of 6.9140mg weretaken and corresponding curves was recorded for $Ce_{0.5}Sr_{0.5}Co_{0.8}Fe_{0.2}O_{3-\delta}$. The TGA curve calculations of samples on this study indicated that the decomposition of calcite occurred at lower temperature. The weight loss is observed three times in the curve. First it was due to evaporation of moisture, second due to evaporation of nitrates and the third due to evaporation of other impurities that comes from the usage of acids and bases (Sharma & Rao, 2015).As it is observed from figure 5, the weight loss is observed three times in the curve. First it was at 124.18°C due to evaporation of moisture, second at 330°C due to evaporation of nitrates and the third at 600°C due to evaporation of other impurities that comes from the usage of acids and bases.

4. Conclusions

$Ce_{0.5}Sr_{0.5}Co_{0.8}Fe_{0.2}O_{3-\delta}$ powders were synthesized by Sol-Gel method and characterized the structural properties. XRD pattern of the samples were taken and the crystallinity nature of the sample observed. SEM and EDS images show the presence of porosity and elemental composition respectively in the samples. The vibrational modes of the molecules or the lattice phonon modes of a crystal were analyzed using Raman spectroscopy and showed that the material is Raman active. The changes of weight in relation to change in temperature were done using TGA-DTA. The pre-sintering and final sintering temperatures of the samples were also decided using the results obtained from TGA-DTA.

Acknowledgements

The authors would like to express their gratitude to department of physics and chemistry of Osmania University for allowing using their laboratory facilities. Finally, we would like to thank ministry of finance of Ethiopia for funding this work.

References

1. Baijnath, Tiwari, P. K., & Basu, S. (2017). Synthesis and performance of $La_{0.5}Sr_{0.5}CoO_3$ cathode for solid oxide fuel cells. *Advanced Materials Letters*, 8, 791-798.
2. Cavallaro, A., Pramana, S. S., Ruiz-Trejo, E., Sherrell, P. C., Ware, E., Kilner, J. A., et al. (2018). Amorphous-cathode-route towards low temperature SOFC. *Sustainable Energy & Fuels*, 4-6.

3. Choi, H., Fuller, A., Davis, J., Wielgus, C., & Ozkan, U. S. (2012). Ce-doped strontium cobalt ferrite perovskites as cathode catalysts for solid oxide fuel cells: Effect of dopant concentration. *Applied Catalysis B: Environmental*, 127, 336–341.
4. Chunwen, S., Rob, H., & Justin, R. (2010). Cathode materials for solid oxide fuel cells: a review. *NRC Publications Archive*, 1125-1144.
5. Dusastre, V., & Kilner, J. A. (1999). Optimization of composite cathodes for intermediate temperature SOFC applications. *Solid State Ionics*, 126, 163-174.
6. Holtappels, P., Vogt, U., & Graule, V. T. (2005). Ceramic materials for advanced solid oxide fuel cells. *Adv. Eng. Mater*, 7, 292-302.
7. Jun, A., Yoo, S., Gwon, O.-h., Shin, J., & Kim, G. (2013). Thermodynamic and electrical properties of $Ba_{0.5}Sr_{0.5}Co_{0.8}Fe_{0.2}O_{3-\delta}$ and $La_{0.6}Sr_{0.4}Co_{0.2}Fe_{0.8}O_{3-\delta}$ for intermediate-temperature solid oxide fuel cells. *Electrochemical Acta*, 89, 372-376.
8. Kuang, K., & Easler, k. (2007). Fuel cells electronics and packaging. 1-32.
9. Kuhn, M., Hashimoto, S., Sato, K., Yashiro, K., & Mizusaki, J. (2013). Thermo-chemical lattice expansion in $La_{0.6}Sr_{0.4}Co_{1-y}FeyO_{3-\delta}$. *Solid State Ionics*, 241, 12-16.
10. Maguire, E., Gharbage, B., Marques, F., & Labrincha, J. (2000). Cathode materials for intermediate temperature SOFCs. *Solid State Ionics*, 127, 329–335.
11. Mai, T. T., Ha, H. K., & Thang, N. M. (2016). Synthesis $La_{0.6}Sr_{0.4}Co_{0.2}Fe_{0.8}O_{3-\delta}$ Perovskite by Microwave Assisted Sol-Gel Method and Properties of LSCF/GDC Composite Cathode for IT-SOFCs. *International Journal of Emerging Research in Management & Technology*, 5, 1-6.
12. Mosiałek, M., Dudek, M., Michna, A., Tatko, M., Kędra, A., & Zimowska, M. (2014). Composite cathode materials Ag- $Ba_{0.5}Sr_{0.5}Co_{0.8}Fe_{0.2}O_3$ for solid oxide fuel cells. *Solid State Electrochem*, 2.
13. Muneeb, I., Khurram, S., Rizwan, R., Anwar, A., Pankaj, T., Bin, Z., et al. (2009). A Brief Description of High Temperature Solid Oxide. *Applied sciences*, 1-23.
14. Ormerod, R. M. (2003). Solid oxide fuel cells. *Chemical Society Reviews*, 32, 17-28.
15. Petric, A., & Tietz, P. H. (2000). A study of ionic materials for the energy applications through first-principles calculations and calphad modeling. *Solid State Ionics*, 719, 1-4.
16. Shao, Z. P., Yang, W. S., Cong, Y., Dong, H., Tong, J. H., & Xiong, G. X. (2001). Operation of perovskite membrane under vacuum and elevated pressures for high-purity oxygen production. *Membrane Science*, 345, 47-52.
17. Shao, Z., & Sossina, M. H. (2004). A high-performance cathode for the next generation of solid-oxide fuel cells. *Nature*, 431, 170-173.
18. Sharma, D. R., & Rao, D. P. (2015). Synthesis and characterization of $Ba_{0.5}Sr_{0.5}(Co_{0.8}Fe_{0.2})_{1-x}Ti_xO_{3-\delta}$ (BSCF) cathode for solid oxide fuel cell. *International Journal of Scientific and Research Publications*, 5, 6-7.
19. Ullmann (2000). High-temperature superconductor materials for contact layers in solid oxide fuel cells. *Solid State Ionics*, 79, 138.
20. Wei, B., Lü, Z., Huang, X., Miao, J., Sha, X., Xin, X., et al. (2006). Crystal structure, thermal expansion and electrical conductivity of perovskite oxides $Ba_xSr_{1-x}Co_{0.8}Fe_{0.2}O_{3-\delta}$ ($0.3 \leq x \leq 0.7$). *Journal of the European Ceramic Society*, 26, 2827–2832.
21. Wincewicz, K. C., & Cooper, J. S. (2005). Fabrication and evaluation of micro tubular solid oxide fuel cell. *Power source*, 140, 280.
22. Yokokawa, H., & Horita, T. (2003). High Temperature Solid Oxide Fuel Cells Fundamentals, Design and Applications. 119.
23. Zhou, W., Ran, R., & Shao, Z. (2009). Progress in understanding and development of $Ba_{0.5}Sr_{0.5}Co_{0.8}Fe_{0.2}O_{3-\delta}$ -based cathodes for intermediate temperature solid-oxide fuel cells: A review. *Journal of Power Sources*, 192, 231-246.
